Structure and Dynamics of Phosphorus(V)-Stabilized Carbanions: A Comparison of Theoretical, Crystallographic, and Solution Structures

Christopher J. Cramer,*,† Scott E. Denmark,*,‡ Paula C. Miller,‡,[1a] Roberta L. Dorow,‡,[1b] Kevin A. Swiss,‡ and Scott R. Wilson‡

Contribution from the Roger Adams Laboratory, Department of Chemistry, University of Illinois, Urbana, Illinois 61801, and Department of Chemistry and Supercomputer Institute, University of Minnesota, 207 Pleasant Street SE, Minneapolis, Minnesota 55455-0431

*Received September 7, 1993**

Abstract: The rotational coordinates about the P–C bond in four different phosphorus(V)-substituted methyl anions have been studied in detail at the HF/3-21G(*) level, with stationary points characterized at levels equivalent to MP3/6-31+G*//HF/6-31+G*. The locations of local minima on the rotational coordinate were found to be dependent on opportunities for hyperconjugative stabilization. When amino substituents on phosphorus were geometrically unconstrained, two local minima were found. By contrast, when the amino groups were constrained to local geometries similar to those found in diazaphosphorinanes, the effects on the rotation coordinate were considerable. A single minimum and a higher rotation barrier were noted. Comparisons of static structure and rotational dynamics are made to both solution and solid-phase experimental data. The single-crystal X-ray structure of lithio-*N,N,N′,N′*-tetramethyl-*P*-benzylphosphondiamide Li^+7^- is reported.

Introduction and Background

In recent years we have been involved in the exploration of the chemistry of phosphorus-stabilized anions.[2] One of the primary goals is the design and development of chirally modified reagents capable of highly stereoselective asymmetric transformations of the anion (e.g., rearrangements, electrophilic substitution) to afford chiral phosphorus[3] and non-phosphorus containing[4] compounds.

The rational design of chiral reagents based on *P*-stabilized anions requires an accurate structural model, one which unfortunately was not available at the outset of our studies.[5] Toward that end, we have initiated and described in preliminary form our first studies on the solution and solid-state structure of *P*-stabilized anions Li^+ 1^- and Li^+ 2^-.[6] Although far from complete, the

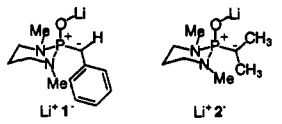

Li^+ 1^- Li^+ 2^-

preliminary picture of the phosphoryl-stabilized anions (phosphondiamides and phosphonates) can be summarized as follows: (1) The anions are planar. (2) There is no metal–carbon contact in ethereal solvents. (3) The lithio anions exist in general as dimers in solution and the solid state. (4) The preferred orientation of the anion is parallel (O–P–C–C, dihedral angle, ca. 180°), and most importantly, (5) the barrier to P–C bond rotation is very low (<8 kcal/mol).

To obtain a better understanding of the magnitude and direction of any intrinsic orientational preferences of the anions, we have chosen to examine the structure, bonding, and P–C rotational coordinates of a number of representative models of phosphoryl-stabilized anions. Detailed descriptions of rotational energetics play a key role in conformational analysis.[7] Indeed, the accurate

† University of Minnesota.

‡ University of Illinois.

* Abstract published in *Advance ACS Abstracts,* February 15, 1994.

(1) (a) Current address: Monsanto Agricultural Company, 800 N. Lindbergh, St. Louis, MO 63167. (b) Current address: Dupont Merck Pharmaceutical Company, DuPont Experimental Station, PO Box 80353, Wilmington, DE 19880.

(2) (a) Denmark, S. E.; Marlin, J. E. *J. Org. Chem.* **1987**, *52*, 5742. (b) Denmark, S. E.; Rajendra, G.; Marlin, J. E. *Tetrahedron Lett.* **1989**, *30*, 2469. (c) Denmark, S. E.; Dorow, R. L. *J. Org. Chem.* **1990**, *55*, 5926. (d) Denmark, S. E.; Stadler, H.; Dorow, R. L.; Kim, J. H. *J. Org. Chem.* **1991**, *56*, 5063. (e) Denmark, S. E.; Chatani, N.; Pansare, S. V. *Tetrahedron* **1992**, *48*, 2191. (f) Denmark, S. E.; Chen, C.-T. *J. Am. Chem. Soc.* **1992**, *114*, 10674. (g) Denmark, S. E.; Amburgey, J. *J. Am. Chem. Soc.* **1993**, *115*, 10386.

(3) (a) Bartlett, P. A.; McLaren, K. L. *Phosphorus Sulfur* **1987**, *33*, 1. (b) Schöllkopf, W.; Schütze, R. *Liebigs Ann. Chem.* **1987**, 45. (c) Ito, Y.; Sawamura, M.; Hayashi, T. *J. Am. Chem. Soc.* **1986**, *108*, 6405. (d) Sting, M.; Steglich, W. *Synthesis* **1990**, 132. (e) Hanessian, S.; Bennani, Y. L.; Delorme, D. *Tetrahedron Lett.* **1990**, *31*, 6461. (f) Hanessian, S.; Bennani, Y. L. *Tetrahedron Lett.* **1990**, *31*, 6465. (g) Genet, J. P.; Uziel, J.; Touzin, A. M.; Juge, S. *Synthesis* **1990**, 41. (h) Togni, A.; Pastor, S. D. *Tetrahedron Lett.* **1989**, *30*, 1071. (i) Vasella, A.; Voeffray, R. *Helv. Chim. Acta* **1982**, *65*, 1953. (j) Sawamura, M.; Ito, Y.; Hayashi, T. *Tetrahedron Lett.* **1989**, *30*, 2247. (k) Jacquier, R.; Ouazzani, F.; Roumestant, M.-L.; Viallefont, P. *Phosphorus Sulfur* **1988**, *36*, 73.

(4) (a) Tömösközi, I.; Janzsó, G. *Chem. Ind. (London)* **1962**, 2085. (b) Bestmann, H. J.; Tömösközi, I. *Tetrahedron* **1968**, *24*, 3299. (c) Bestmann, H. J.; Heid, E.; Ryschka, W.; Lienert, J. *Justus Liebigs Ann. Chem.* **1974**, 1684 and references cited therein. (d) Trost, B. M.; Curran, D. P. *J. Am. Chem. Soc.* **1980**, *102*, 5699. (e) Johnson, C. R.; Elliott, R. C.; Meanwell, N. A. *Tetrahedron Lett.* **1982**, *23*, 5005. (f) Hanessian, S.; Delorme, D.; Beaudoin, S.; Leblanc, Y. *J. Am. Chem. Soc.* **1984**, *106*, 5754. (g) Hanessian, S.; Delorme, D.; Beaudoin, S.; Leblanc, Y. *Chem. Scr.* **1985**, *25*, NS5. (h) Hua, D. H.; Chan-Yu-King, R.; McKie, J. A.; Myer, L. *J. Am. Chem. Soc.* **1987**, *109*, 5026. (i) Gais, H.-J.; Schmiedl, G.; Ball, W. A.; Bund, J.; Hellmann, G.; Erdelmeier, I. *Tetrahedron Lett.* **1988**, *29*, 1773. (j) Rehwinkel, H.; Skupsch, J.; Vorbrüggen, H. *Tetrahedron Lett.* **1988**, *29*, 1775. (k) Takahashi, T.; Matsui, M.; Maeno, N.; Koizumi, T.; Shiro, M. *Heterocycles* **1990**, *30*, 353. (l) Polniaszek, R. P.; Foster, A. L. *J. Org. Chem.* **1991**, *56*, 3137. (m) Harmat, N. J. S.; Warren, S. *Tetrahedron Lett.* **1990**, *31*, 2743. (n) Hanessian, S.; Beaudoin, S. *Tetrahedron Lett.* **1992**, *33*, 7655. (o) Hanessian, S.; Beaudoin, S. *Tetrahedron Lett.* **1992**, *33*, 7659.

(5) For early investigations on the structure of *P*-stabilized anions, see: (a) Seyden-Penne, J. *Bull. Soc. Chim. Fr.* **1988**, 238. (b) Strzalko, T.; Seyden-Penne, J.; Froment, F.; Corset, J.; Simonnin, M.-P. *J. Chem. Soc., Perkin Trans. 2* **1987**, 783. (c) Strzalko, T.; Seyden-Penne, J.; Froment, F.; Corset, J.; Simonnin, M.-P. *Can. J. Chem.* **1988**, *66*, 391. (d) Teulade, M.-P.; Savignac, P.; About-Jaudet, E.; Collignon, N. *Phosphorus Sulfur* **1988**, *40*, 105. See also: (e) Corset, J. *Pure Appl. Chem.* **1986**, *58*, 1133. (f) Patios, C.; Ricard, L.; Savignac, P. *J. Chem. Soc., Perkin Trans. 1* **1990**, 1577.

(6) (a) Denmark, S. E.; Dorow, R. L. *J. Am. Chem. Soc.* **1990**, *112*, 864. (b) Denmark, S. E.; Miller, P. C.; Wilson, S. R. *J. Am. Chem. Soc.* **1991**, *113*, 1468. (c) Denmark, S. E.; Swiss, K. A.; Wilson, S. R. *J. Am. Chem. Soc.* **1993**, *115*, 3826. (d) Denmark, S. E.; Swiss, K. A. *J. Am. Chem. Soc.* **1993**, *115*, 12195.

0002-7863/94/1516-2437$04.50/0

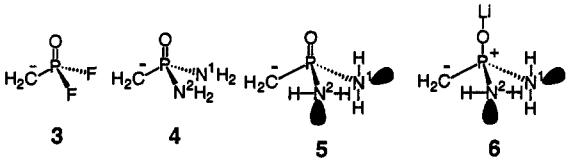

3 4 5 6

Figure 1. Four phosphorus(V)-stabilized anions addressed computationally.

description of torsional motions is integral to the success of force-field molecular mechanics techniques.[8] For small molecules in the gas phase, both spectroscopic and theoretical studies have provided considerable insight into rotational barriers.[9] Of course, for the phosphoryl-stabilized anions, experimental access to this information is very challenging and the complexity of these molecules prohibits gas-phase measurements. Solution-phase dynamic NMR spectroscopy[10] is the method of choice, and we have already made use of these measurements.[6] Nevertheless, there remain sufficient experimental limitations that detailed geometrical information is not always available.

On the other hand, ab initio theoretical methods have been applied with considerable success to describe negatively charged compounds containing third-row elements.[11] Moreover, theoretical methods do not suffer from the experimental difficulties that set practical limits on the smallest magnitude rotational barrier which may be observed, and the fundamental, electronic nature of a single rotation may readily be probed. While it is recognized that the results of gas-phase calculations will only semiquantitatively describe the state of affairs in solution, differential solvation effects on rotamers may be expected to be fairly small in the absence of carbon–metal contacts, as observed for the phosphoryl-stabilized anions discussed here.[6a,b] We have recently reported the first ab initio calculations of phosphorus(V)-stabilized anions (allyl anions) and have shown that the structures were in good agreement with the results of solution-phase spectroscopic studies.[11c]

We present here a theoretical study of the rotational coordinates for four different phosphorus(V)-stabilized carbanions (Figure 1).[12] The methylphosphonic difluoride anion (**3**) is particularly simple and serves as a first-order model. Since our synthetic studies have focused predominantly on phosphonamide derivatives,[2] the methylphosphondiamide anion (**4**) is chosen as a more relevant model. Recognizing the importance of nitrogen lone-pair orientations to the electronic character of chiral phosphorus groups, we additionally focus on conformers of **4** where the amino groups are artificially constrained. In these species, the H–N–P angles, the N–P–N angle, and the H–N–P–O dihedral angles are frozen at values taken from X-ray crystal structure determinations of the cyclic diazaphosphorinane-derived anions.[6a,b] This conformer of **4** will be referred to as **5** for clarity. Finally, the lithiated version of **5** (referred to as **6**) is studied, where the lithium atom is collinear with the P–O bond and coordinated to oxygen. This species **6** (conformationally constrained as well) is a monomeric simplification based on the solid-state structures of lithiophosphonamides that also have no carbon–lithium contacts (vide infra).

Anion **4** has already been cursorily studied by Frenking, Boche, et al.,[12] who identified two local minima related as P–C bond rotamers at the HF/3-21G(*) level in the context of a more detailed study of the anion of methylphosphonate (i.e., $^-CH_2P(O)(OH)_2$). The details of the phosphondiamide structures will be discussed more fully below. The analysis of Frenking, Boche, et al. was limited primarily to (1) noting the nearly degenerate energies of the two minima for **4** and (2) noting that one of the minima was in reasonable accord with an extant X-ray crystal structure of a phosphondiamide-stabilized anion.[6a]

Our purpose here is to perform a much more detailed analysis of the rotational coordinate about the P–C bond, to include identifying and quantifying torsional barriers, and to elucidate the fundamental features of the molecular electronic structure which control the rotational energetics. We combine this analysis with low-temperature dynamic NMR studies in ethereal solvents, and finally we also report the third in a series of X-ray crystallographic structure determinations of lithiated phosphondiamides to facilitate comparisons to the results of the calculations. We compare both the present and earlier[11c] related theoretical studies with several solid-state structures. Using these three diverse methods, we achieve a coherent understanding of the features controlling the stereochemistry, and thereby the synthetic utility, of phosphondiamide-stabilized carbanions.

Computational Methods

For **3** and **4**, all structures on the P–C bond rotation coordinate were fully optimized with respect to all remaining degrees of freedom at the HF/3-21G(*) level of theory.[13] Compounds **5** and **6** were optimized at the same level, additionally constraining the H–N–P angles and H–N–P–O dihedrals to be identical to those from the solid-state structure of lithio-2-benzyl-1,3-dimethyl-1,3,2-diazaphosphorinane 2-oxide (Li^+ **1**$^-$).[6a] Further, P–O–Li collinearity was enforced in **6**. Stationary points on the rotation coordinate were optimized with no rotational constraint and characterized by inspection of appropriate Hessian matrices. All stationary points (for **5** and **6** "stationary" clearly refers to a reduced-dimensionality hypersurface which lacks the frozen degrees of freedom) were additionally optimized at either the HF/6-31G*, HF/6-31+G*, or HF/6-31+G*(*) levels.[14] The (*) in the latter basis set implies addition of a set of p orbitals (exponent 1.1) to the methylene hydrogen atoms but not to those on the amino groups. Single-point second- (MP2) and third-order (MP3) Møller–Plesset many-body perturbation theory (frozen core)[15] was employed to account for electron correlation at the 6-31+G* level (**3**), the 6-31+G*(*) level (**4** and **5**), and the 6-31G*(*) level (**6**). Analytic frequency analysis for **3** was performed within the rigid-rotor, harmonic oscillator approximation at the HF/6-31+G* level. Zero-point vibrational energies (ZPVE) were calculated after scaling all frequencies by 0.89. All calculations utilized the GAUSSIAN 88 suite of programs.[16]

Experimental Methods

General Methods. For a recent description of the general synthetic methods see ref 2d. The X-ray structural details of Li^+ **1**$^-$ and Li^+ **2**$^-$ have been reported previously.[6a,b] Benzylphosphonic dichloride was

(7) Eliel, E. L.; Allinger, N. L.; Angyal, S. J.; Morrison, G. A. *Conformational Analysis*; Wiley-Interscience: New York, 1965.

(8) (a) Allinger, N. L.; Grev, R. S.; Yates, B. F.; Schaefer, H. F., III. *J. Am. Chem. Soc.* **1990**, *112*, 114 and references therein. (b) Bowen, J. P.; Allinger, N. L. In *Reviews in Computational Chemistry*; Lipkowitz, K. B., Boyd, D. B., Eds.; VCH: New York, 1991; Vol. 2, p 81.

(9) Burbert, W.; Allinger, N. L. *Molecular Mechanics*; American Chemical Society: Washington, DC, 1982.

(10) (a) Fraenkel, G.; Hsu, H.; Su, B. M. In *Lithium: Current Applications in Science, Medicine and Technology*; Bach, R. O., Ed.; Wiley: New York, 1985; p 273. (b) Brown, T. L. *Adv. Organomet. Chem.* **1965**, *3*, 365. (c) Jackman, L. M.; Lange, B. M. *Tetrahedron* **1977**, *33*, 2737.

(11) (a) Streitwieser, A., Jr.; Williams, J. E., Jr. *J. Am. Chem. Soc.* **1975**, *97*, 191. (b) Schleyer, P. v. R.; Clark, T.; Kos, A. J.; Spitznagel, G. W.; Rohde, G.; Arad, D.; Houk, K. N.; Rondan, N. G. *J. Am. Chem. Soc.* **1984**, *106*, 6467. (c) Denmark, S. E.; Cramer, C. J. *J. Org. Chem.* **1990**, *55*, 1806. (d) Dahlke, G. D.; Kass, S. R. *J. Am. Chem. Soc.* **1991**, *113*, 5566. (e) Peräkylä, M.; Pakkanen, T. A.; Björkroth, J.-P.; Pohjala, E.; Leiras, H. O. *J. Chem. Soc., Perkin Trans. 2* **1992**, 1167.

(12) While this work was in progress we became aware of similar calculations on the anions of methylphosphonic acid and methylphosphondiamide. Our results are in good agreement with calculations by these investigators. We are grateful to Professor Gernot Boche for a preprint of this manuscript. Zarges, W.; Marsch, M.; Harns, K.; Haller, F.; Frenking, G.; Boche, G. *Chem. Ber.* **1991**, *124*, 861.

(13) Pietro, W. S.; Francl, M. M.; Hehre, W. J.; DeFrees, D. J.; Pople, J. A.; Binkley, J. S. *J. Am. Chem. Soc.* **1982**, *104*, 5039.

(14) (a) Francl, M. M.; Pietro, W. J.; Hehre, W. J.; Binkley, J. S.; Gordon, M. S.; DeFrees, D. J.; Pople, J. A. *J. Chem. Phys.* **1982**, *77*, 3654. (b) Frisch, M. J.; Pople, J. A.; Binkley, J. S. *J. Chem. Phys.* **1984**, *80*, 3265.

(15) (a) Møller, C.; Plesset, M. S. *Phys. Rev.* **1934**, *46*, 618. (b) Pople, J. A.; Seeger, R.; Krishnan, R. *Int. J. Quantum Chem., Symp.* **1977**, *11*, 49.

(16) Frisch, M. J.; Head-Gordon, M.; Schlegel, H. B.; Raghavachari, K.; Binkley, J. S.; Gonzalez, C.; DeFrees, D. J.; Fox, D. J.; Whiteside, R. A.; Seeger, R.; Melius, C. F.; Baker, J.; Martin, R. L.; Kahn, L. R.; Stewart, J. J. P.; Fluder, E. M.; Topiol, S.; Pople, J. A. *Gaussian 88*; Gaussian Inc.: Pittsburgh, PA, 1988.

Table 1. Selected Bond Lengths (Å) and Angles (deg) for **3–6**

	3[a,b]		**4**[c,d] (C_1)		**4**[c,d] (C_s)		**5**[c,d]		**6**[c,d]	
atoms	minimum	saddle pt	minimum	saddle pt	minimum	saddle pt	minimum	saddle pt	minimum	saddle pt
					Lengths					
P–O	1.467	1.470	1.483	1.483	1.487	1.488	1.490	1.485	1.521	1.528
P–C	1.660	1.693	1.687	1.700	1.695	1.677	1.697	1.708	1.653	1.655
P–X(1)	1.605	1.591	1.726	1.703	1.696	1.715	1.722	1.691	1.685	1.666
P–X(2)	1.605	1.591	1.695	1.705	1.696	1.715	1.715	1.715	1.671	1.693
					Angles					
O–P–C	121.9	129.6	117.4	121.8	130.3	117.8	120.6	125.0	115.4	122.1
O–P–X(1)	108.9	106.5	103.6	108.5	104.0	109.9	104.7	108.7	102.0	105.7
O–P–X(2)	108.9	106.5	116.1	107.8	104.0	109.9	112.5	107.4	111.7	104.9
C–P–X(1)	110.8	106.0	118.5	108.5	103.7	110.2	113.9	104.9	118.8	108.6
C–P–X(2)	110.8	106.0	104.4	108.7	103.7	110.2	102.9	107.3	107.0	112.2
X(1)–P–X(2)	91.0	98.0	95.2	99.2	110.6	96.7	101.1	101.1	101.1	101.1

[a] Calculated at the HF/6-31+G* level. [b] X = F. [c] Calculated at the HF/6-31+G*(*) level. [d] X = N.

prepared by modification of the literature procedure.[17] NMR data are reported in ppm; coupling constants are in hertz; IR data are in cm^{-1}; mass spectral data are given as m/z.

***N,N,N',N'*-Tetramethylbenzylphosphondiamide (7).** Diethyl ether saturated with dimethylamine (4 mL) was introduced to a 25-mL, three-necked flask equipped with a stirring bar, a rubber septum, and a N_2 inlet. Diethyl ether (10 mL) was added, and the solution was cooled in an ice bath. Triethylamine (1 mL, 7.2 mmol, 5.1 equiv) was added via syringe. A solution of benzylphosphonic dichloride (295 mg, 1.41 mmol) in diethyl ether (5 mL) was added to the solution dropwise via syringe (a white precipitate formed immediately). The solution was warmed to room temperature and was stirred for 6 h. The suspension was filtered and concentrated to give a white crystalline solid. The crude product was purified by silica gel chromatography using EtOAc/hexane, 1/1, to give 215 mg (67%) of **7** as a white solid. The product was then recrystallized from hexane to give 199 mg (62%) of a white crystalline solid: mp 79.5–80.5 °C (hexane); ^{1}H NMR (300 MHz, $CDCl_3$) 7.27 (m, 5 H, aromatic protons), 3.21 (d, J_{PH} = 16.2, 2 H, $H_2C(1)$), 2.54 (d, J_{PH} = 9.4, 12 H ($(CH_3)_2N)_2$); ^{13}C NMR (75.5 MHz, $CDCl_3$) 133.07 (d, J = 7.6, C(2)), 129.77 (d, J = 5.2, C(3) and C(7)), 128.31 (d, J = 2.3, C(5)), 126.41 (d, J = 2.8, C(4) and C(6)), 36.10 (d, J = 2.6, C(8–11)), 33.20 (d, J = 108.9, C(1)); ^{31}P NMR (121.4 MHz, $CDCl_3$) 34.67; IR (KBr) 3060 (w), 3031 (w), 2984 (m), 2890 (m), 2803 (m), 1601 (w), 1495 (w), 1455 (m), 1294 (s), 1204 (s, P=O), 1136 (w), 1069 (w), 982 (s); MS (70 eV) 227 (M^+ + 1, 1.56), 226 (M^+, 12), 135 (100), 92 (13), 91 (30), 44 (30); TLC R_f = 0.44 (EtOAc/hexane, 1/1). Anal. Calcd for $C_{11}H_{19}N_2OP$: C, 58.39; H, 8.46; N, 12.38; P, 13.69. Found: C, 58.32; H, 8.46; N, 12.34; P, 13.72.

Lithio-*N,N,N',N'*-Tetramethylbenzylphosphondiamide (Li^+ 7^-). *N,N,N',N'*-Tetramethylbenzylphosphondiamide (21.5 mg, 0.10 mmol) was introduced into a flame-dried test tube (5 mm × 50 mm) fitted with a rubber septum and a nitrogen inlet (syringe needle). Anhydrous THF (110 μL) was added via syringe, and the resulting solution was cooled in a –78 °C bath. *tert*-Butyllithium (1.50 M in pentane, 70 μL, 0.11 mmol, 1.1 equiv) was added dropwise via syringe (final concentration 0.53 M). The yellow solution was frozen in liquid nitrogen to initiate crystallization and then stored in a freezer (ca. –20 °C). Clear, colorless crystals formed over a 12–16-h period. For the crystal mounting and diffraction experimental details see supplementary material.

Results

Theoretical Structures of 3–6. A. Stationary Points. While the various stationary points characterized for the phosphonyl-stabilized methyl anions **3–6** are of particular interest to us in the context of P–C bond rotation, as discussed more fully below, there are additional features exhibited by these structures which merit separate discussion; we present certain details here.

Two stationary points were located for the methylphosphonic difluoride anion (**3**). The conformation of the global minimum exhibits a parallel anion (i.e., the P=O bond is eclipsed by one of the C—H bonds) and is of C_s symmetry. A saddle point, also of C_s symmetry, was located which corresponds to a 90° torsion about the P—C bond relative to the minimum; i.e., now it is the carbanion lone pair which eclipses the P=O bond. Selected structural details from the highest level optimizations are presented in Table 1 and Figure 2. Several comparisons are interesting, both between these two anionic structures themselves and as well to the structure of neutral ethylphosphonic difluoride.[18] First, upon formation of the anion, the P=O bond lengthens by about 0.03 Å, the P—C bond shortens by a dramatic 0.13 Å, and the P—F bonds lengthen by roughly 0.05 Å compared to those bonds in ethylphosphonic difluoride. In addition, the O—P—C bond angle widens by roughly 3°. Comparing the two anion structures, on passing from the minimum to the saddle point, the P=O and P—C bonds both become slightly longer, while the P—F bonds contract by a similar amount. More noticeable is a large increase, on the order of 7 to 8°, in both the O—P—C and F—P—F bond angles.

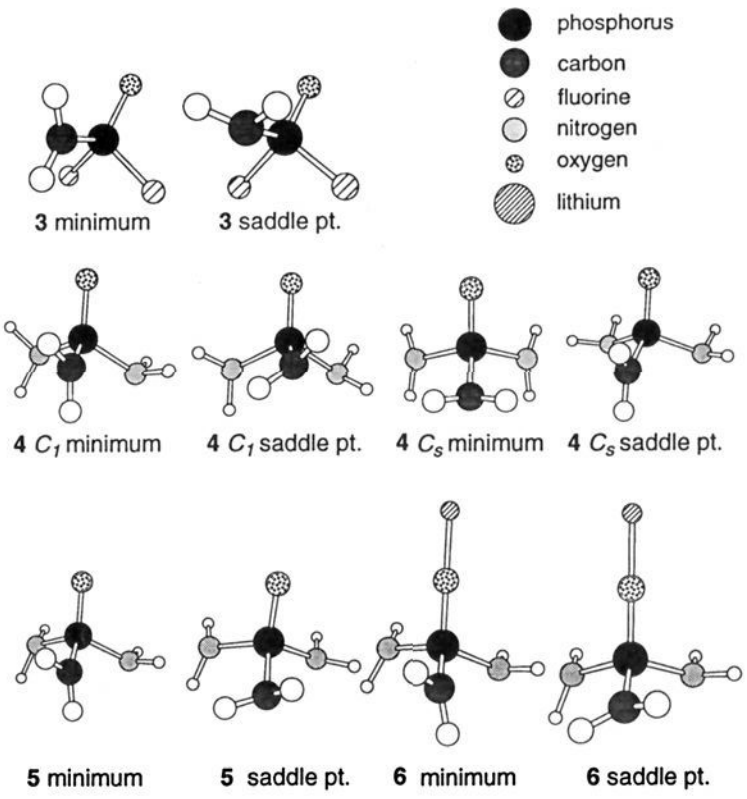

Figure 2. Chem 3D representations of the theoretical stationary points for **3–6**.

Two stationary points for the methylphosphonic diamide anion (**4**) are reminiscent of the above structures for **3**, except that in this case both are local minima (Table 1). Just as was observed for **3**, upon going from the C_1 minimum with an approximately parallel anion to the C_s minimum with a perpendicular anion, there is a lengthening of the P=O and P—C bonds and a large widening of the O—P—C and N—P—N bond angles. Additionally, *one* of the P—N bonds shortens, as observed for the P—F case; however, the other remains unchanged. Again comparing to the uncharged precursor,[11c,12] there is an increase

(17) (a) Bhongle, N. N.; Notter, R. H.; Turcotte, J. G. *Synth. Commun.* **1987**, *17*, 1071. (b) McKenna, C. E.; Miza, M. T.; Cheung, N. H.; McKenna, M. C. *Tetrahedron Lett.* **1977**, 155.

(18) Durig, J. R.; Hizer, T. J.; Harlan, R. J. *J. Phys. Chem.* **1992**, *96*, 541.

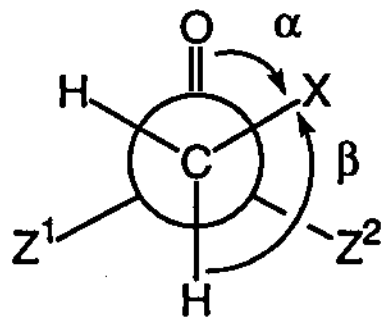

Figure 3. Definitions for the geometrical descriptors α and β. X is an imaginary substituent, α is depicted as positive, and β is always taken to be positive.

in P=O bond length (~0.015 Å) and P—N bond lengths (0.04 to 0.07 Å), a shortening of the P—C bond (~0.12 Å), and an opening of the O—P—C bond angle. These results for the minima agree with those reported earlier by Frenking, Boche, et al.[12] There are additionally two saddle points, one of C_1 and one of C_s symmetry, which exhibit geometries roughly intermediate between those of the two minima (Table 1).

Finally, the analogs of **4** in which the amino groups have been constrained to resemble the appropriate portions of a diazaphosphorinane ring are similar in many respects to the other anions. Both the free anion (**5**) and the lithiated anion (**6**) have a single local minimum equilibrium structure and a single saddle point, the two systems resembling each other quite closely (Table 1). Moreover, they are additionally close in resemblance to the parallel and perpendicular minima and saddle points already mentioned for **3** and **4**, with bond length and bond angle changes on interconversion mimicking those detailed above (with the exception, of course, of the frozen N—P—N bond angle). The gross geometry of **5** is quite similar to that of **4**, in particular with regard to the much shorter P—C bond than found in neutral phosphonic diamides.[11c,12] In **6**, on the other hand, there are a few particularly noticeable changes upon lithiation, viz., the sizable lengthening of the P=O bond (0.03–0.04 Å) with concomitant shortening of the P—C and P—N bonds by about the same amount relative to **5**. In addition, the O—P—C and O—P—X bond angles decrease by up to 5°.

A detailed analysis of these trends is facilitated by examination of how these various stationary points fit into the overall P—C torsional coordinate, to which we now turn our attention.

B. Rotational Coordinates. Since the methylene anion is conformationally variable with respect to its inversion mode, the rotational coordinate is poorly described by torsional angles involving one of the methylene hydrogens. We define instead the torsional angle α, where α represents the dihedral angle ω(O–P–C–X) and X is an imaginary carbanion substituent which lies in the plane bisecting the H–C–H angle and containing the P–C bond (Figure 3). Furthermore, α will be defined as positive in a left-handed screw sense when sighting down the C–P bond. As a descriptor for the relative planarity/pyramidality, we define β as the dihedral angle between the two planes defined by atoms H, C, and P and atoms X, C, and P, respectively. By construction, this dihedral is identical to within sign for the two methylene hydrogen atoms; hence, we will always take it to be positive. It is apparent by inspection that a perfectly planar carbanion will then have $\beta = 90°$ and a pyramidal anion $\beta = 60°$ or 120° (assuming all tetrahedral angles).[19] It is further evident from consideration of local and molecular symmetry that the complete rotational coordinate is described by $0° \leq \alpha < 180°$ for **3** and potentially **4** (vide infra) and by $0° \leq \alpha < 360°$ for **5** and **6**, where the two amino groups cannot be enantiotopically related by virtue of their constrained geometries.

In addition, we have found that, for a given value of α, there is only a single value of β which delivers a reduced-dimensionality stationary point; i.e., *there are never two stable pyramidal carbanions related by inversion of the carbanionic center.* This reduces the rotational coordinate for **3** to $0° \leq \alpha \leq 90°$ and for **5** and **6** to $0° \leq \alpha < 180°$. Compound **4** is a special case which is discussed below.

Thus, for each of **3–6**, α was stepped through its required range by increments of 15°. For **3**, as mentioned above, the local minimum occurs for the C_s $\alpha = 90°$ structure, and the barrier is described by the C_s $\alpha = 0°$ structure. Relative energies together with geometrical descriptors may be found in Table 2, and the rotational coordinate is illustrated in Figure 4.

For **4** the situation is more subtle. There is a C_s global minimum at $\alpha = 0°$, a nonsymmetric barrier at $\alpha = 36.9°$, and a second minimum at $\alpha = 69.9°$. The lowest energy $\alpha = 90°$ structure, however, does *not* possess C_s symmetry. Although the methylene is nearly planar, the amino groups are quite differently oriented relative to the C–P–O plane. Continued rotation of the methylene in very small increments increases the energy and causes the amines to rotate counter to each other. By following the S-shaped minimum-energy path[20] on the complete hypersurface, one may

Table 2. Relative Energies and β Values for **3–6** as a Function of α[a,b]

	3		4		5		6	
α	E_{rel}[c]	β	E_{rel}[d]	β	E_{rel}[e]	β	E_{rel}[f]	β
0	6.57[g]	82.0	0.00	75.8	5.50	72.4	6.45	85.2
15	6.01	85.4	0.81	75.7	4.33	75.5	4.78	87.7
30	4.44	89.3	2.85	76.4	2.70	83.9	2.70	91.4
			(3.92[g]	81.4)[h]				
45	2.49	92.3	2.64	88.9	0.95	91.1	0.86	93.8
60	0.96	92.8	1.33	92.4	(0.00	93.9)[i]	(0.00	94.2)[j]
75	0.19	91.9	(1.13[k]	93.8)[l]	0.36	93.9	0.49	93.3
90	0.00	90.0	1.93[m]	92.5	1.63	91.9	1.96	90.7
			3.63[g]	90.0				
105					3.19	88.1	3.67	87.0
120					4.69	86.9	5.25	85.0
135					6.04	91.9	6.69	85.9
150					(6.69[g]	102.5)[n]	7.58	90.0
							(7.66[g]	91.7)[o]
165					6.40	106.8	7.46	93.9

[a] Calculated at the HF/3-21G(*) level. [b] Relative energies in kcal/mol, α and β in deg. [c] Relative to –650.299 88 au. [d] Relative to –563.002 14 in kcal/mol, α and β in deg. [e] Relative to –562.994 58 au. [f] Relative to –570.473 47 au. [g] Saddle point (rotation barrier). [h] $\alpha = 36.9°$. [i] $\alpha = 63.5°$. [j] $\alpha = 62.1°$. [k] Local minimum. [l] $\alpha = 69.9°$. [m] C_1 nonstationary point. [n] $\alpha = 151.8°$. [o] $\alpha = 155.8°$.

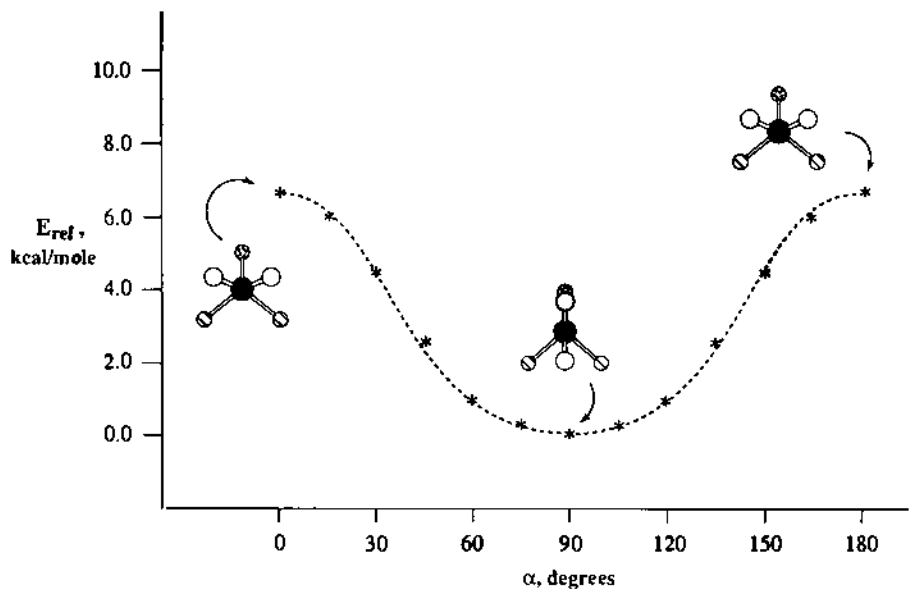

Figure 4. Relative energy in kcal/mol for **3** vs carbanion rotation angle α at the HF/3-21G(*) level. Illustrated stationary points were optimized at the HF/6-31+G* level (see Tables 1–3). For atom-label legend see Figure 2.

(19) For visualization, it is convenient to regard X as a "point-lone-pair" and take the P–C–X "bond angle" to be ca. 90°. However, as long as P, C, and X are noncollinear, the dihedral angles are constant for any PCX angle.

(20) Such "S-curves" are not uncommon, see: (a) Mezey, P. G. *Potential Energy Hypersurfaces*; Elsevier: Amsterdam, 1987. (b) Clark, T. *A Handbook of Computational Chemistry*; Wiley-Interscience: New York, 1985; p 187.

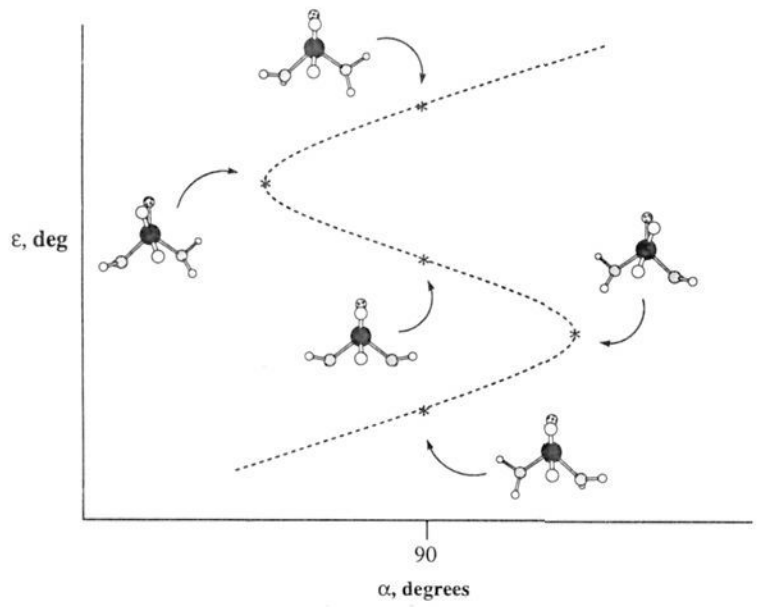

Figure 5. Energy of **4** with respect to α. This is not well-defined in the vicinity of $\alpha = 90°$. Consideration of amine rotation is required to adequately describe the carbanion rotation. The coordinate ϵ represents some generalized coordinate for amino group rotation. Energy decreases continuously as one travels down the path from the C_s symmetric midpoint in either direction. For atom-label legend see Figure 2.

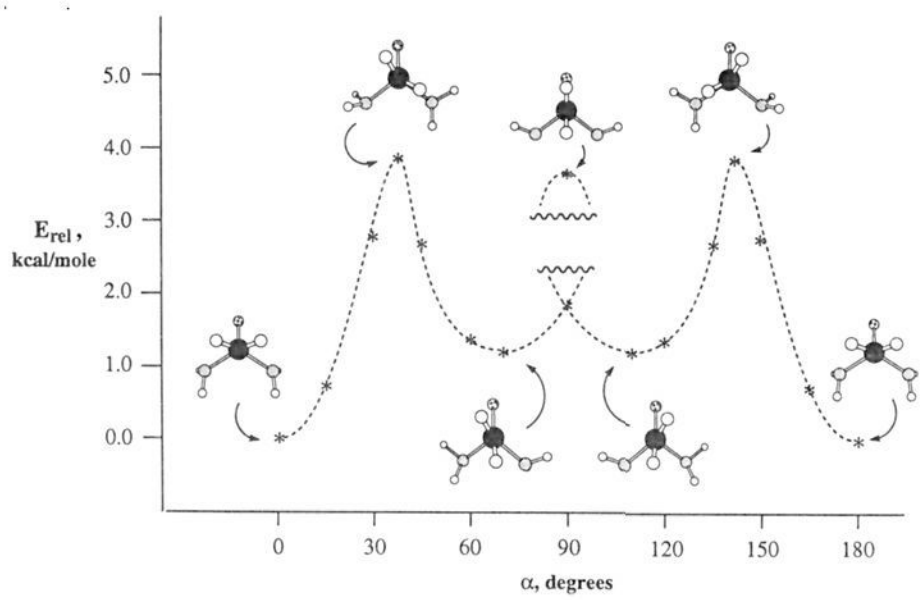

Figure 6. Relative energy in kcal/mol for **4** vs carbanion rotation angle α at the HF/3-21G$^{(*)}$ level. Illustrated stationary points were optimized at the HF/6-31+G*$^{(*)}$ level (see Tables 1–3). For atom-label legend see Figure 2.

arrive at a second rotation barrier (one negative force constant) which *is* C_s and lies slightly higher in energy than the nonsymmetric $\alpha = 90°$ structure; i.e., the barrier separates the two enantiomeric forms of the C_1 minimum. It follows that projection of the complete hypersurface onto the rotational coordinate does not give a unique energy value for α near 90°; the latter requires specification of an additional molecular coordinate. This process is illustrated in Figure 5. The data for the overall rotation are presented in Table 2 and Figure 6.

For **5** and **6**, no ambiguity in α arises, since the amino groups are locked, thus artificially reducing their contribution to the dimensionality of the hypersurface. This facilitates the location of rotational minima and saddle points. The global minimum for **5** is at $\alpha = 63.5°$, and the barrier of 6.7 kcal/mol occurs at $\alpha = 151.8°$. Lithiation at oxygen has relatively little effect on the shape of this curve (the minimum moves to $\alpha = 62.1°$ and the barrier to $\alpha = 155.8°$) but does raise the magnitude of the barrier to 7.7 kcal/mol. The data and structures are found in Table 2 and Figures 7 and 8.

Additionally, all stationary points on the rotation coordinates were further optimized at the Hartree–Fock level with larger and more flexible basis sets. These data are collected in Table 3.

X-ray Crystallographic Analysis of Li$^+$ 7$^-$. We have previously reported the solid-state structures of Li$^+$ **1**$^-$ and Li$^+$ **2**$^-$.[6a,b] The details of these structures are quite similar (not surprisingly in retrospect). Most striking among the similarities were (1) the near planarity of the anionic carbons, (2) the torsional preferences about the P–C bond, and (3) the pyramidalization of the nitrogens. To probe whether these similarities were due to unique features of the 1,3,2-diazaphosphorinane ring unit, we chose to examine an analogous *P*-benzylphosphondiamide anion not constrained to a cyclic structure. We were pleased to find that the simplest representative of this class, Li$^+$ **7**$^-$, was a well-behaved species that could be studied spectroscopically[21] and that further could be coaxed to crystallize suitably for X-ray analysis.

The anion crystallized as a tetra-THF-solvated dimer in which the two subunits were related by an inversion center. There are two dimeric moieties in the unit cell (Table 4). ORTEP representations of the dimeric and monomeric units are depicted in Figure 9. Key bond lengths, bond angles, and torsion angles are collected in Table 5.

The basic features of the solid-state structure are quite similar to those of the previously described lithio-*P*-benzyl-1,3,2-diazaphosphorinane 2-oxide (Li$^+$ **1**$^-$).[6a] Both molecules crystallized as C_i symmetric dimers with four additional THF molecules attached to the Li–O–Li–O rhombus. There is clearly no carbon–lithium contact, as judged by the 3.678(6)-Å distance between C(1) and Li(1) (compare to 3.83(1) Å in Li$^+$ **1**$^-$). The rehybridization of the carbanion is very similar in the two species, as is evident in the length of the C(1)–P(1) bond (1.683(3) Å

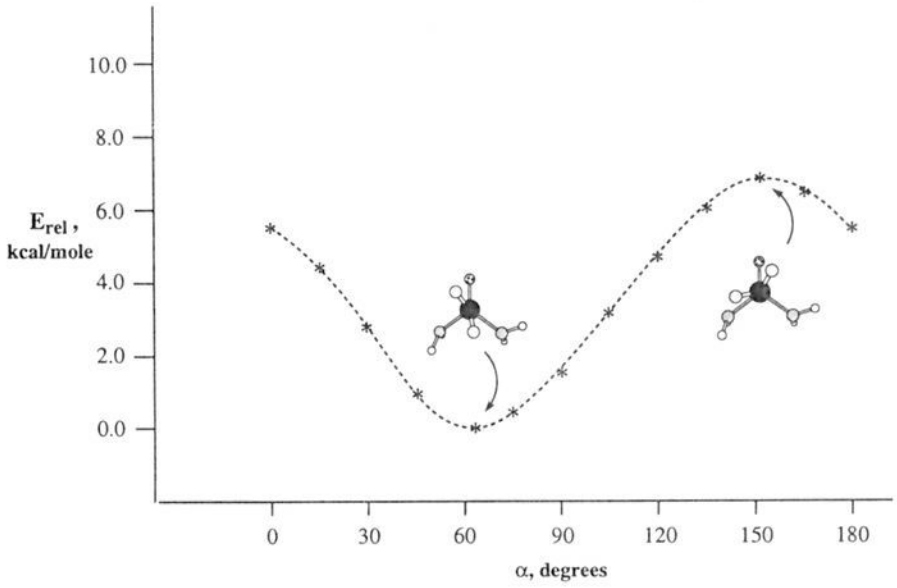

Figure 7. Relative energy in kcal/mol for **5** vs carbanion rotation angle α at the HF/3-21G$^{(*)}$ level. Illustrated stationary points were optimized at the HF/6-31+G*$^{(*)}$ level (see Tables 1–3). For atom-label legend see Figure 2.

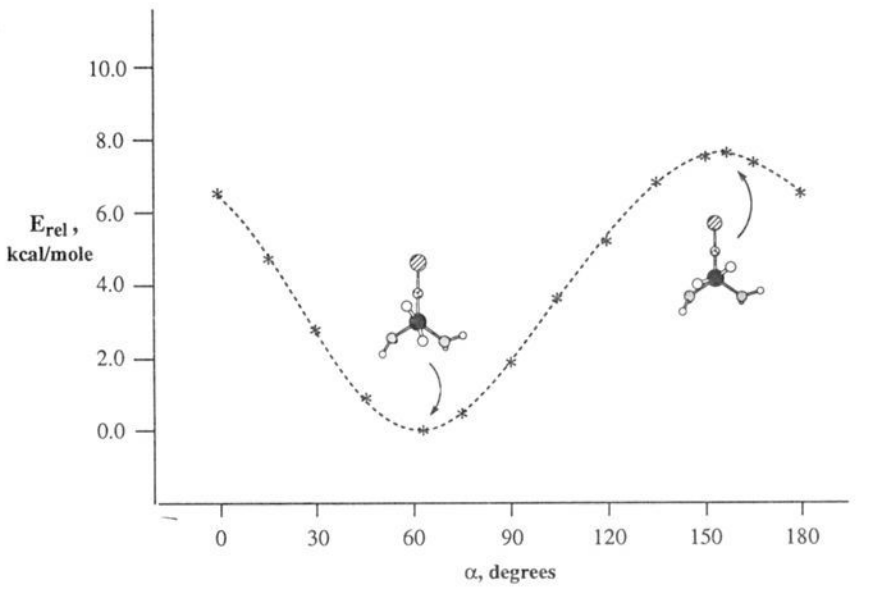

Figure 8. Relative energy in kcal/mol for **6** vs carbanion rotation angle α at the HF/3-21G$^{(*)}$ level. Illustrated stationary points were optimized at the HF/6-31+G*$^{(*)}$ level (see Tables 1–3). For atom-label legend see Figure 2.

(21) The details of the solution structure of Li$^+$ **7**$^-$ will be described in a forthcoming full account of our structural studies: Denmark, S. E.; Swiss, K. A.; Dorow, R. L.; Miller, P. C.; Wilson, S. R. Manuscript in preparation.

Table 3. Absolute and Relative Energies and α and β Values for 3–6 Optimized at Various Theoretical Levels[a]

		3			4			5			6		
level	point[b]	E	α	β	E	α	β	E	α	β	E	α	β
HF/6-31G*	GM	−653.57324	90.0	90.0	−565.83615	70.9	106.7	−565.82707	65.8	107.8	−573.32097	63.8	100.9
	LM				1.37	0.0	66.5						
	TS1	5.82	0.0	65.3	2.71	90.0	90.0	6.60	139.4	117.2	8.70	152.5	98.9
	TS2				3.42	46.4	69.4						
HF/6-31+G*(*)[c]	GM	−653.60112	90.0	90.0	−565.86937	72.6	102.2	−565.86139	67.2	104.3	−574.02335	64.6	100.1
	LM				0.90	0.0	69.2						
	TS1	6.19	0.0	66.6	2.91	90.0	90.0	7.27	145.7	115.0	9.30	154.5	99.5
	TS2				2.98	44.7	74.7						
MP2[d]	GM	−654.39179			−566.65804			−566.65094			−574.09114		
	LM				0.75								
	TS1	5.81			3.46			8.34			8.80		
	TS2				3.14								
MP3[d]	GM	−654.38950			−566.67791			−566.67032			−574.11635		
	LM				0.85								
	TS1	5.91			3.35			7.93			8.74		
	TS2				3.13								
ZPVE[e]	GM	20.11											
	TS	19.97											

[a] Absolute energies for global minima are in au; relative energies for other isomers and ZPVE are in kcal/mol; α and β are in deg. [b] GM = global minimum, LM = local minimum, TS1 = first saddle point, TS2 = second saddle point. [c] For 4–6 a set of p functions was added to the methylene hydrogens. [d] Single-point calculations, levels are MPx/6-31+G*//HF/6-31G* for 3, MPx/6-31+G*(*)//HF/6-31+G*(*) for 4 and 5, and MPx/6-31G*(*)//HF/6-31+G*(*) for 6. [e] Calculated at the HF/6-31+G* level.

Table 4. Crystal and Experimental Data for Li^+ 7^-

crystal system	monoclinic
space group	$P2_1/n$
a, Å	9.641(5)
b, Å	14.346(5)
c, Å	15.192(3)
β, deg	91.71(2)
V, Å^3	2100(2)
Z	2
ρ (calcd), g/cm^3	1.190
temperature, °C	−100
color, habit	colorless, transparent, prismatic
dimensions, mm	0.20 × 0.30 × 0.50
diffractometer, radiation	Enraf-Nonius CAD4, Mo($\kappa\bar{\alpha}$)
μ, cm^{-1}	1.45
2θ limit, deg (octants)	50.0 ($-h+k\pm l$)
intensities measd (unique)	4188 (3688)
intensities > $2.58\sigma(I)$	2340
R	0.046
R_w (for $w = 1.89/(\sigma^2(F_o) + pF_o^2)$)	0.047 ($p = 0.01$)
density range in ΔF map, e/Å^3	+0.40 to −0.44

compared to 1.689(5) Å in Li^+ 1^-). The carbanionic center C(1) is nearly perfectly planar by at least four criteria of planarity, even more so than in the case of Li^+ 1^- (see Discussion). For example, the distance of C(1) from the plane defined by H(1)–P(1)–C(2) is only 0.010 Å in Li^+ 7^- compared to 0.056 Å in Li^+ 1^-. In addition, the conformation of the benzyl group with respect to the phosphonamide moiety is strikingly similar in both compounds. The diagnostic dihedral angle O(1)–P(1)–C(1)–C(2) is 159.8(3)° in Li^+ 7^- compared to 168.9(3)° in Li^+ 1^-. It is noteworthy that the deviation from idealized coplanarity (180°) arises from a similar type of distortion relating to the disposition of the phosphonamide nitrogens.

One of the most striking features of Li^+ 1^- was the pyramidalization of the nitrogens (from initially planar nitrogens in 1). Moreover the pyramidalization was unsymmetrical, resulting in a chiral anion with one axial and one equatorial methyl group ascribed as a consequence of an anomeric effect through phosphorus.[22] In Li^+ 7^- on the other hand the nitrogens (no longer constrained in a ring) are nearly planar, as judged by the sum of the angles: $\Sigma_{(angle)}$ N(1) 359.3°; N(2) 357.3°. Still more remarkable than the planarity of the nitrogen groups is their mutually orthogonal dispostion. By the definition of α in Figure 3, the plane of the N(1) dimethylamino unit is canted 17° off normal to the P(1)–O(1) vector while the plane of the N(2) dimethylamino unit is perfectly normal to the P(1)–N(1) vector, (see Figure 9 monomer unit). These orientations are symptomatic of the unique stereoelectronic features of the phosphonamide unit, as discussed below.

Discussion

Theoretical Stationary Points. Many of the geometrical consequences of anion formation in the theoretical structures for 3–6 are in good agreement with earlier spectroscopic[6a,b] and theoretical studies.[11c,12] In particular, the significant shortening of the P—C bond and lengthening of the P═O bond relative to the case of the uncharged species upon formation of the anion have been interpreted to imply that the C—P—O linkage becomes much more ionic in character, i.e. $^-$C—P$^+$—O$^-$, where the charge separation lengthens the P═O bond slightly because of loss of double-bond character but shortens the P—C bond because of increased ionic interactions.[6,11c] The effect of lithiation at oxygen is consistent with this rationalization. Polarization of the negative charge from oxygen to lithium further decreases the P—O interaction, and that bond lengthens. By so doing, the remaining ionic interactions between P—C and P—N are increased, and these bonds shorten. Finally, this analysis also affords some insight into the large increase in the C—P—O angle observed upon passing from a parallel anion conformation to a perpendicular one. In the latter instance, the carbanionic lone pair eclipses the similarly electron-rich P—O system; the resulting repulsion forces the angle to widen.

There is probably an additional component to this bond angle widening, which further plays a role in the F—P—F and N—P—N bond angle changes observed in 3 and 4 upon passing from the parallel to the perpendicular anion. Once again, however, the explication is clarified by considering these issues within the context of torsional motion about the P—C bond.

Theoretical Rotational Coordinates. By comparison of Figures 4 and 6–8, it is evident that lithiation of 5 to produce 6 has little

(22) (a) Reed, A. E.; Schleyer, P. v. R. *J. Am. Chem. Soc.* **1987**, *109*, 7362 and references therein. (b) Cramer, C. J. *J. Am. Chem. Soc.* **1991**, *113*, 2439. (c) Wang, P.; Zhang, Y.; Glaser, R.; Reed, A. E.; Schleyer, P. v. R.; Streitwieser, A. *J. Am. Chem. Soc.* **1991**, *113*, 55. (d) Uchimaru, T.; Tanabe, K.; Nishikawa, S.; Taira, K. *J. Am. Chem. Soc.* **1991**, *113*, 4351. (e) Dejaegere, A.; Lim, C.; Karplus, M. *J. Am. Chem. Soc.* **1991**, *113*, 4353. (f) Setzer, W. N.; Bentrude, W. G. *J. Org. Chem.* **1991**, *56*, 7212. (g) Wang, P.; Zhang, Y.; Glaser, R.; Streitwieser, A.; Schleyer, P. v. R. *J. Comput. Chem.* **1993**, *14*, 522. (h) Cramer, C. J.; Gustafson, S. M. *J. Am. Chem. Soc.* **1993**, *115*, 9315. (i) Cramer, C. J.; Gustafson, S. M. *J. Am. Chem. Soc.* **1994**, *116*, 723.

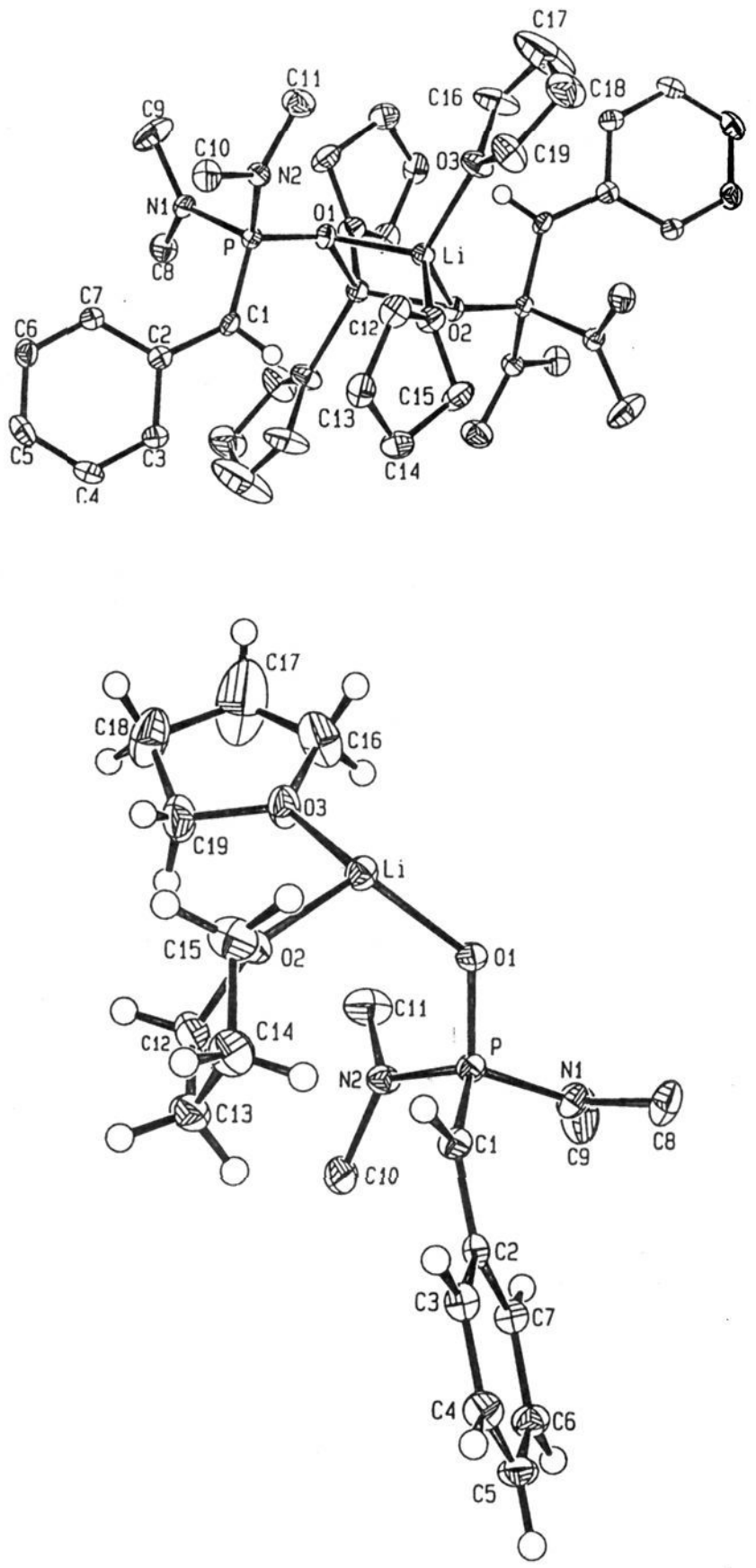

Figure 9. ORTEP representations (35% probabililty ellipsoids) of the dimer and monomer units of Li^+ 7^-.

effect on the rotation coordinate as a whole.[23] The local minimum and the barrier are shifted slightly from those for the free anion. The energetics are similar, but the barrier for **6** was raised 1 kcal/mol relative to that for **5**. The rotational coordinate for **3** is also quite similar in energetics to **5** and **6**, although it is shifted out of phase by roughly 30°. Anion **4**, on the other hand, has a profile remarkably different from that of the other three. Most striking is the local minimum at $\alpha = 0°/180°$.

It is instructive to compare as well the β vs α profiles for the four compounds. Here, except for the extradimensional S-curve arising from coupled amino rotation near $\alpha = 90°$, **4** behaves quite similarly to the remaining substrates. The parameter β behaves exactly as one would expect. Rather than eclipsing filled bond orbitals, the carbanion lone pair inverts (i.e., β passes through 90°) so as always to be antiperiplanar to the most nearly parallel bond. This is illustrated in Figure 10 for the particular case of **3**; the other cases are all qualitatively similar.

(23) It must be stressed that the 3-21G(*) basis set surfaces under discussion give results for the rotational coordinate that are only qualitative, especially for the charged species. However, computation of the nonstationary points on the curves at the much higher levels employed for the local minima and saddle points would be prohibitively costly and provide little additional insight. Keeping in mind the more accurately described stationary points from the higher level calculations and accepting that the general appearance of the rotational coordinates would be slightly changed, we will continue the discussion at this lower level.

Table 5. Selected Bond Lengths, Bond Angles, and Torsional Angles for Li^+ 7^-

Bond Lengths, Å					
P(1)–O(1)	1.520(2)	C(1)–C(2)	1.425(4)	N(1)–C(8)	1.449(4)
P(1)–N(1)	1.665(3)	O(1)–Li(1)	1.935(5)	N(1)–C(9)	1.436(5)
P(1)–N(2)	1.669(3)	O(1)–Li(1)[a]	1.926(5)	N(2)–C(10)	1.451(4)
P(1)–C(1)	1.683(3)	O(2)–Li(1)	1.959(6)	N(2)–C(11)	1.458(4)
		O(3)–Li(1)	1.979(6)		

Bond Angles, deg			
O(1)–P(1)–C(1)	111.9(1)	P(1)–N(1)–C(8)	118.9(2)
O(1)–P(1)–N(1)	112.3(1)	P(1)–N(1)–C(9)	126.1(2)
O(1)–P(1)–N(2)	105.3(1)	C(8)–N(1)–C(9)	114.3(3)
C(1)–P(1)–N(1)	109.0(1)	P(1)–N(2)–C(10)	120.5(2)
C(1)–P(1)–N(2)	113.9(1)	P(1)–N(2)–C(11)	122.6(2)
N(1)–P(1)–N(2)	104.3(1)	C(10)–N(2)–C(11)	114.2(3)
P(1)–C(1)–C(2)	131.9(2)	O(1)–Li(1)–O(2)	116.0(3)
P(1)–C(1)–H(1)	112(2)	O(1)–Li(1)–O(3)	114.5(3)
H(1)–C(1)–C(2)	116(2)	O(2)–Li(1)–O(3)	101.8(3)
		O(1)–Li(1)–O(1)[a]	95.0(2)

Torsional Angles, deg			
O(1)–P(1)–C(1)–C(2)	−159.8(3)	O(1)–P(1)–N(2)–C(10)	−160.9(2)
O(1)–P(1)–N(1)–C(8)	+68.4(3)	O(1)–P(1)–N(2)–C(11)	+38.8(3)
O(1)–P(1)–N(1)–C(9)	−101.6(3)	P(1)–C(1)–C(2)–C(3)	+175.4(3)

[a] Equivalent position $(-x, -y, -z)$.

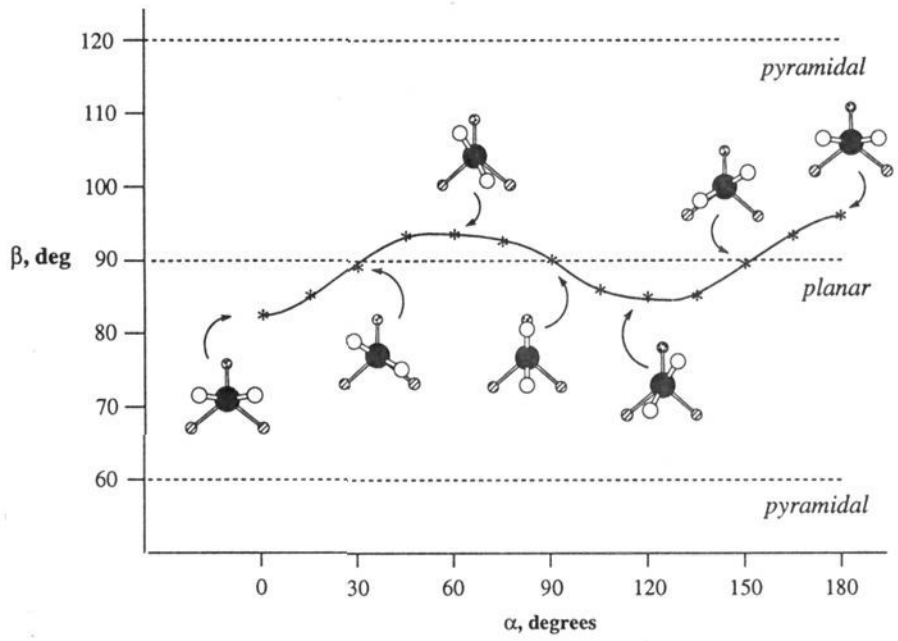

Figure 10. Carbanion pyramidality descriptor β vs carbanion rotation angle α for **3** at the HF/3-21G(*) level (see Table 2). Higher level calculations for stationary points exhibit more pronounced pyramidality at carbon (see Table 3). For atom-label legend see Figure 2.

Not surprisingly, all of the local minima in **4**–**6** occur for structures having essentially perfect antiperiplanarity between the carbanionic lone pair and one of the P–X bonds. For **3**, symmetry considerations give rise to a structure midway between the two possible P–F anti conformations. It appears that there is some unique factor in **4** which makes antiperiplanarity of the anion to the P–O bond favorable, since none of the others exhibit a local minimum at that point. In addition, **5** and **6** enjoy an energy minimum when the carbanion is anti to only *one* amino group, not the other.

Postponing briefly a discussion of the anomalies, these conformational energetics are reminiscent of the anomeric effect, first observed in the context of carbohydrate chemistry.[24] In a generalized sense, the anomeric effect rationalizes stabilization of an antiperiplanar bond–lone-pair type structure by invoking a favorable delocalization of the lone pair, which need not be anionic, into the empty σ^* orbital of the acceptor bond. Supporting

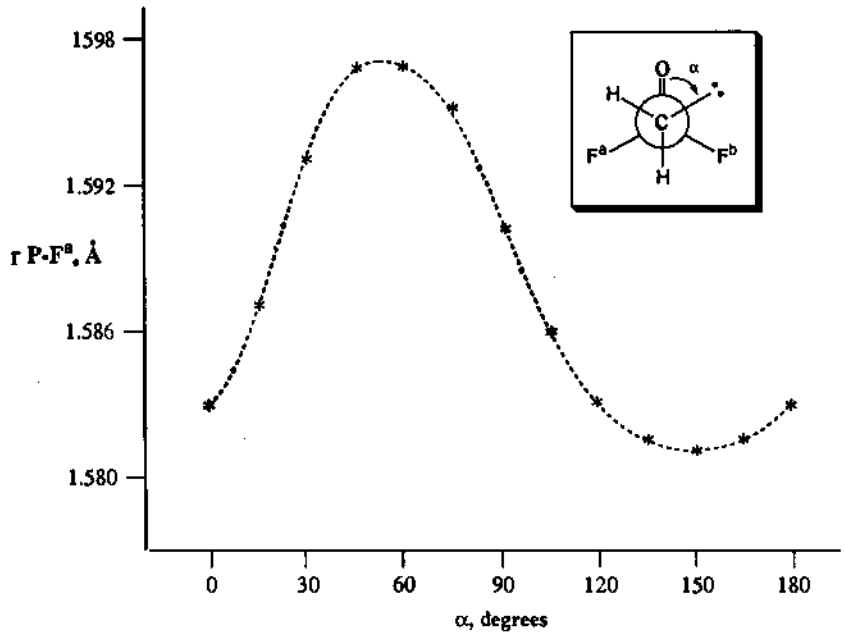

Figure 11. P–F^a bond length vs carbanion rotation angle α for **3** at the HF/3-21G$^{(*)}$ level. The bond is at its longest when the carbanion is anti to it and at its shortest when the carbanion is orthogonal to it.

evidence for such an electronic redistribution of charge is the lengthening of the acceptor bond upon adoption of the anomerically stabilized conformation. Figure 11 depicts one of the P–F bond lengths in **3** as a function of α, and indeed the bond lengthens as the carbanionic lone pair becomes antiperiplanar and contracts when it is perpendicular.[25,26] Another hallmark of the anomeric effect is the widening of bond angle between the three atoms involved upon hyperconjugative stabilization. This is the additional component to the increase in C–P–O bond angle mentioned earlier. The widening occurs upon passing from the parallel anion, which has minimal opportunity to delocalize the carbanion into the σ^*_{P-O} orbital, to the perpendicular, where the overlap is much better. Although it is not possible to uniquely separate bond angle widening into electrostatic and hyperconjugative components, overall it is clear that hyperconjugative interactions are playing an important role in the electronic structure of these anions.

Generalized anomeric effects through phosphorus have been noted before.[22] Indeed, by Fourier decomposition of the potential surface for internal rotation,[27] Gordon et al. assigned such hyperconjugation to be the dominant factor in the rotation energetics of phosphinous acid (H_2POH).[28] Cramer has observed a similar situation for the open-shell hydroxyphosphoranyl (H_3POH),[29] while Uchimaru et al.[22d] and Dejaegere et al.[22e] have discussed this effect for intermediates in phosphate hydrolysis. It thus remains only to explain why certain conformations in **3**–**6**, which would appear at first glance to be anomerically stabilized, are not.

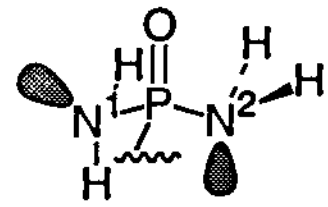

Figure 12. Illustration of the orientation of the nitrogen lone pairs when the amino groups are constrained to a diazaphosphorinane-like geometry.

A comparison of the four acceptor σ^*_{P-X} bond orbitals available in **5** (and **6**) within the context of *all* possible anomeric delocalizations provides considerable insight. Figure 12 illustrates the situation for the phosphondiamide fragment in the constrained, diazaphosphorinane-like geometry. One nitrogen atom, N(2), has its lone pair pseudo-axially disposed, such that anomeric delocalization into the σ^*_{P-O} orbital may occur. The other, N(1), has its lone pair disposed pseudo-equatorially and is thus able to take advantage of $\sigma^*_{P-N(2)}$ delocalization. Consistent with this analysis is the 8–10° larger O–P–N(2) bond angle (indicating anomeric stabilization) compared to the O–P–N(1) bond angle in the minima for **5** and **6** (Table 1). Oxygen lone-pair delocalization is fairly evenly distributed into the two σ^*_{P-N} and the σ^*_{P-C} orbitals, since the lone-pair density about oxygen is approximately cylindrically symmetric about the P–O axis.[30] There is thus an overall *dearth* of delocalization into the $\sigma^*_{P-N(1)}$ orbital in the diazaphosphorinane-like fragment. *It is exactly that rotamer which allows maximum carbanionic delocalization into this orbital which is the local minimum for* **5** *(and* **6***).* Once again, the 11 to 12° larger bond angle for the C–P–N(1) linkage compared to the C–P–N(2) unit is indicative of anomeric stabilization occurring. Finally, the point on the rotation coordinate where the carbanionic lone pair is orthogonal to the $\sigma^*_{P-N(1)}$ orbital corresponds to the rotation barrier.

In **4**, the above-discussed "propeller-like" arrangement of lone pairs is observed for the *non*-symmetric local minimum. However, the rotational mobility of the amino groups allows for *other* situations where each lone pair may enjoy delocalization into a unique σ^*_{P-X} orbital. Thus, rotation of the amino group with lone pair anti to oxygen, coupled with a counter-rotation of the carbanion, amounts to these two lone pairs swapping the antibonding orbitals with which they interact. This delivers the C_s local minimum at $\alpha = 0°$. This analysis also provides an explanation for the S-curve in the hypersurface near $\alpha = 90°$. In order for each of the two possible rotamers placing the carbanion anti to a nitrogen atom to be local minima, they must have enantiomeric, propeller-like arrangements of their lone pairs. If methylene rotation were not coupled with amino rotation, the carbanion could still be rotated to be anti to the *second* nitrogen atom, but the resulting conformer would have no lone pair anti to the *first* nitrogen atom. It is evident from consideration of **5** and **6** that such a situation does *not* deliver a local minimum.

These hyperconjugative arguments also explain such features as the very large N–P–N bond angle for the C_s local minimum compared to the C_1 minimum. Since only in the former is anomeric stabilization occurring within the N–P–N linkage, it is entirely consistent that this trend is observed. Similarly, it is only in the latter rotamer that an $n_N \rightarrow \sigma^*_{P-O}$ delocalization occurs, and for that delocalization alone is a large O–P–N angle observed (116.1°) compared to all of the others in either minima (103.8 ± 0.2°).

(24) (a) Kirby, A. J. *The Anomeric Effect and Related Stereoelectronic Effects at Oxygen*; Springer Verlag: Berlin, 1983. (b) Riddell, F. G. *The Conformational Analysis of Heterocyclic Compounds*; Academic Press: New York, 1980; pp 66–103. (c) Deslongchamps, P. *Stereoelectronic Effects in Organic Chemistry*; Pergamon Press: Oxford; U.K., 1983. (d) Romers, C.; Altona, C.; Buys, H. R.; Havinga, E. *Top. Stereochem.* **1969**, *4*, 39. (e) Szarek, W. A.; Horton, D. *Anomeric Effect, Origin and Consequences*; ACS Symposium Series 87; *American Chemical Society*; Washington, DC, 1979. (f) Box, V. G. S. *Heterocycles* **1990**, *31*, 1157. (g) Juaristi, E. *Acc. Chem. Res.* **1989**, *22*, 357. (h) Cramer, C. J. *J. Org. Chem.* **1992**, *57*, 7034.

(25) Since the anion inverts, the P–F bond is never eclipsed.

(26) Wiberg has questioned such an interpretation in different systems, suggesting instead that bonding electron density is polarized away from the vicinity of the lone pair, giving rise to lengthened bonds without requiring lone-pair delocalization. However, this argument was introduced for molecules where the proposed acceptor orbital was σ^*_{X-H}, e.g., methylamine. The acceptor qualities of the σ^*_{P-X} orbitals involved here are much improved over those of the σ^*_{X-H} orbitals considered by Wiberg. Wiberg, K. B. *J. Am. Chem. Soc.* **1990**, *112*, 3379.

(27) (a) Radom, L.; Hehre, W. J.; Pople, J. A. *J. Am. Chem. Soc.* **1972**, *94*, 2371. (b) Veillard, A. *Chem. Phys. Lett.* **1969**, *4*, 51. (c) Salzner, U.; Schleyer, P. v. R. *J. Am. Chem. Soc.* **1993**, *115*, 10231.

(28) Schmidt, M. W.; Yabushita, S.; Gordon, M. S. *J. Phys. Chem.* **1984**, *88*, 382.

(29) (a) Cramer, C. J. *J. Am. Chem. Soc.* **1990**, *112*, 7965. (b) The situation is similar for a thiol substituent. Cramer, C. J. *Chem. Phys. Lett.* **1993**, *202*, 297.

(30) The convention of using a "double" bond to describe the dative bonding between phosphorus and oxygen in phosphorus(V) compounds arises from consideration of dissociation energies relative to phosphorus(III) "true" P–O single bonds. It has been shown repeatedly, however, that the electronic nature of the bond does not involve only a single π_{p-p}-type interaction. See, for instance: (a) Schmidt, M. W.; Gordon, M. S. *Can. J. Chem.* **1985**, *63*, 1609. (b) Schmidt, M. W.; Gordon, M. S. *J. Am. Chem. Soc.* **1985**, *107*, 1922. (c) Wallmeier, H.; Kutzelnigg, W. *J. Am. Chem. Soc.* **1979**, *101*, 2804.

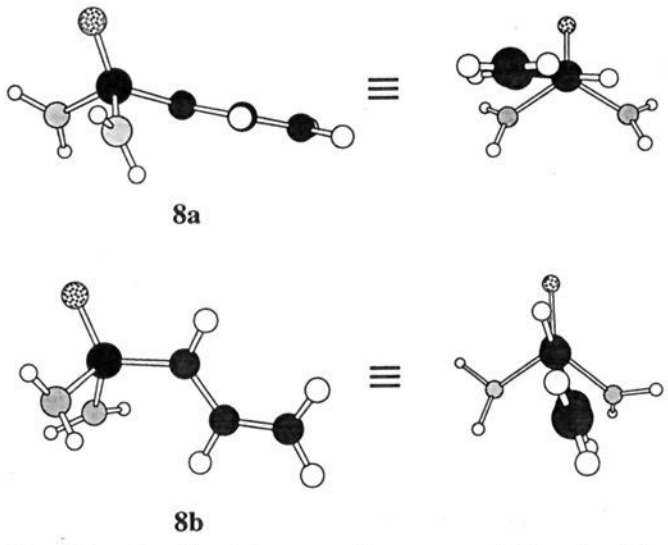

Figure 13. Two local minima analogous to **4** for the *E*-anion of *P*-allylphosphonic diamide at the HF/3-21G(*) level.

Finally, for **3**, the fluorine atoms give rise to a slightly different situation. Since fluorine lone-pair density is approximatelycylindrically symmetric about the axes of the P–F bonds, the phosphonic difluoride fragment has no σ^* orbital which "lacks" partial occupation. For the carbanion, then, it is simply a question of which rotamer enjoys the most stabilization. It is not surprising that the carbanion prefers delocalization into the symmetric combination of σ^*_{P-F} orbitals given the greater electronegativity of fluorine compared to oxygen.

The barriers to P–C bond rotation in these molecules, then, occur for conformations midway between equivalent or nonequivalent local minima, where anomeric stabilization of the carbanion is at a minimum (albeit still probably nonzero). It is thus unsurprising that the saddle points for **3**, **5**, and **6** are of higher relative energy than those for **4**. For the former cases, the carbanionic lone pairs are orthogonal to the best acceptor orbitals, whereas for the latter ones there is at most at a 30° dihedral to favorable acceptor orbitals. For **3**, **5**, and **6**, there are also energetic contributions from the effect of P–C bond rotation on the molecular dipole moment. This dipolar contribution is expected to be quite small, since in **6**, for instance, the dipole moments for the local minimum and the rotameric saddle point are 9.6 and 10.3 D, respectively, i.e., a change of less than 10%. With its conformationally mobile amino groups, there is no correlation of dipole moment (evaluated at the center of mass) and relative energies for P–C bond rotamers in **4**. Thus, hyperconjugation appears to be far and away the chief energetic influence on these rotational coordinates.

Our work with **4** caused us to reexamine an earlier published study on the *P*-allylphosphonic diamide anion (**8**).[11c] While we successfully located an analogous $\alpha = 0°$ local minimum in this molecule (**8a**), as well as a C_s $\alpha = 90°$ rotation barrier, we did not find a C_1 local minimum analogous to $\alpha = 69.9°$ in **4**. Armed with the data from **4**, we were able to subsequently find such a local minimum for **8**, with $\alpha = 71.9°$ and $\beta = 92.0°$ (**8b**), lying 0.5 kcal/mol above the $\alpha = 0°$ rotamer (Figure 13). The orientation of the amino groups is exactly as expected. While it is possible that two other local minima exist, related to these two by exchange of the vinyl group with the hydrogen attached to that anionic center, we have not attempted to locate them. We have discussed E/Z isomerism elsewhere.[11c]

As a final computational point, we note that use of improved basis sets and inclusion of electron correlation affect the various species differently (Table 3). At the 3-21G(*) level, there is probably a fair amount of "borrowing" by other atoms of phosphorus basis functions, since it is the only heavy atom on which d functions are found. Thus, especially for the charged species, an anomalous amount of what appears to be $p\pi$–$d\pi$ bonding is expected (so-called basis set superposition error). However, improving the basis by adding polarization and diffuse functions results only in small effects on both the relative energies

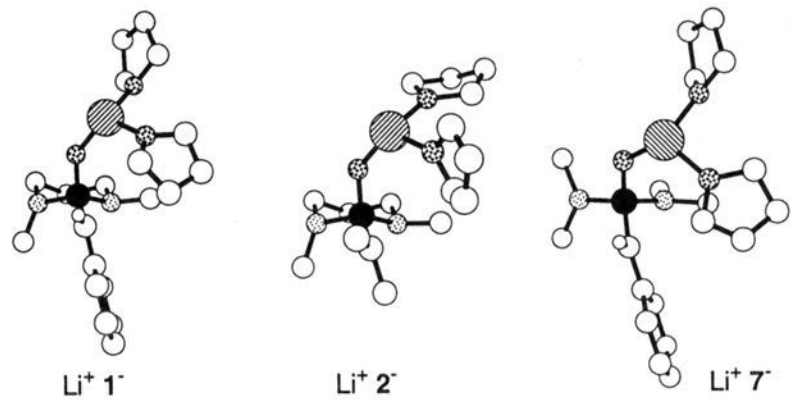

Figure 14. Chem 3D representations of the X-ray crystal structures of Li^+ **1**$^-$, Li^+ **2**$^-$, and Li^+ **7**$^-$; monomer units shown for clarity .

and the angles α observed for the stationary points of **3**–**6**. While these changes are modest, their occurrence in opposite directions *does* give rise to a switch in the relative stabilities of the two local minima for **4**.

This basis set effect is *not* small, however, when considering the parameter β. As expected, removal of anomalous π overlap contributes to dramatically increased pyramidalization of the carbanion in **3**–**5**. In addition, it is well-established that polarization functions (i.e., d functions) are required on nitrogen to accurately reproduce pyramidality at that atom.[31] As expected, then, the amino groups go from being almost perfectly planar at the 3-21G(*) level to being significantly pyramidalized with the more complete basis set. In this regard, the present calculations improve upon those of Frenking, Boche, et al.[12] Diffuse functions, on the other hand, induce slightly decreased pyramidality at the carbanionic center. These effects at carbon are less pronounced in **6**, as expected for an uncharged molecule. Inclusion of correlation effects at the MP2 level gives additional modest changes in relative energies, with again a switch in relative stability occurring, now for the two saddle points of **4**. By the MP3 level, the estimated correlation energies appear to be approaching convergence. Finally, the difference between the zero-point vibrational energies for the minimum and saddle point conformers of **3** is negligible. It is reasonable to expect that the relative energies of the phosphondiamide congeners will be similarly unperturbed.

Comparison to X-ray Crystallographic Data. It is instructive to compare our theoretical results with data from single-crystal X-ray structures determined for three different lithiated phosphondiamide derivatives. Shown in Figure 14 are "front-view" projections of the monomer units of Li^+ **1**$^-$, Li^+ **2**$^-$, and Li^+ **7**$^-$. This graphical depiction clearly shows the similarity in the structures, in particular the key elements of carbanion hybridization and conformation, and the disposition of the nitrogen atoms. A comparison of the three crystal structures with the theoretical structures assessing various criteria of carbanion planarity and disposition is presented in Table 6 along with the definitions of these criteria. In addition, a comparison of key bond lengths for the lithio anion **6** and the crystallographically determined data is provided.

While basic structural differences make quantitative comparisons of geometrical details unrealistic, some trends are especially noteworthy. The theoretical structure of the methyl anion **6** is remarkably similar in the basic bonding details to the crystallographically determined structures. Most notable is how well the significant shortening of the P–C bond in the anions is also seen in the computational minimum. Further, the modest lengthening of the P–O bond is also found. Finally, a trend in the difference between the P–N(1) and P–N(2) bond lengths is accurately predicted computationally. In all three crystal structures, the P–N(1) bond is slightly longer than the P–N(2) bond. This was ascribed to the hyperconjugative stabilization of

(31) Rauk, A.; Allen, L. C.; Clementi, E. *J. Chem. Phys.* **1970**, *52*, 4133.

Table 6. Comparison of Calculated Minimum-Equilibrium Structures with Single-Crystal X-ray Structures[a,b]

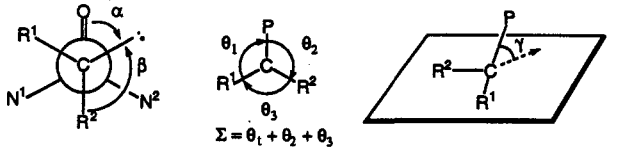

$\Sigma = \theta_1 + \theta_2 + \theta_3$

compound	bond lengths, Å P–O	P–C	P–N(1)	P–N(2)	α, deg	β, deg	Σ, deg	γ, deg
Li^+ 1^-[d]	1.516	1.689	1.681	1.675	74.5	94.5	359.4	7.3
Li^+ 2^-[e]	1.525	1.657	1.708	1.697	67.1	97.3	358.5	11.6
4[c]					72.6	102.2	351.5	19.7
5					67.2	104.3	353.8	23.6
6	1.521	1.653	1.685	1.671	64.6	100.1	357.5	15.9
Li^+ 7^-	1.520	1.683	1.669	1.665	69.0	90.9	360.0	1.3
8a[c]					71.9	92.0	359.9	3.1

[a] Equilibrium minima for **4–6** calculated at the HF/6-31+G*(*) level. [b] See Figure 14 for X-ray structures. [c] Only the C_1 local minimum is presented. [d] Reference 6a. [e] Reference 6b.

the carbanion into the $\sigma^*_{P-N(1)}$ orbital and is manifest nicely in the theoretical structure as well.

The next fundamental structural attribute to be considered is the degree of planarity observed for the carbanions in the solid state. Recall that for β, a value of 90° implies perfect planarity and a value of 120° signifies pyramidality with all tetrahedral angles between substituents. The degree of planarity observed in these systems is not merely a function of benzylic ($p\pi$–$p\pi$) conjugation, as β for Li^+ 2^- (97.3°) is a mere 2.8° larger than that for Li^+ 1^- (94.5°). This stands in contrast to a similar lithioisopropylphenylsulfone, where β is 110.5°.[32] By all criteria Li^+ 7^- contains the most planar carbanion.

Theory does well at reproducing all of the planarity measures. Comparing **6** (which is lithiated) with Li^+ 2^-, there is only a 2.3° difference in β. With **4** and **5**, slightly greater pyramidality is observed. As discussed above, this would probably decrease if more diffuse functions were added to better disperse the full negative charge in these unlithiated models. Additionally, Li^+ 1^-, Li^+ 7^-, and **8** are more nearly planar than either **4**, **5**, **6**, or Li^+ 2^-, as expected for the π-conjugated anions.

More striking still is the excellent correlation between theory and experiment with respect to the conformation of the carbanion. A common feature of all of the crystal structures is the preference for a roughly parallel orientation of the anion as indicated by the O(1)–P(1)–C(1)–C(2) torsional angle. For the purposes of comparison this feature is designated by the carbanionic lone-pair orientation, as described by α. In spite of the many simplifications used in the theoretical models, this *dihedral* angle spans a mere 10° across all seven compounds. As described above, the preferred orientation of the carbanion is dictated by the potential for carbanionic lone-pair overlap with the $\sigma^*_{P-N(1)}$ orbital. This is clearly seen in the canting of the benzyl and isopropyl groups in Figure 14 and from the similarity of the α values in the 65–75° range. Thus, the hyperconjugative stabilization invoked by analysis of the theoretical results both here and elsewhere[22,29] seems to be operative in the solid state as well.

It is also tempting to speculate on the origin of the orthogonal disposition of the nitrogen groups in Li^+ 7^-. Planarity notwithstanding, the propeller-like arrangement of the lone pairs in Li^+7^- is roughly mimicked by the C_1 global minimum for **4** (E_{rel} = 0.0 kcal/mol at all levels above HF/3-21G(*)). The crystal structure embodies the complementarity of hyperconjugative overlap ($n_{C(1)} \rightarrow \sigma^*_{P-N(2)}$; $n_{N(1)} \rightarrow \sigma^*_{P-O(1)}$; and $n_{N(2)} \rightarrow \sigma^*_{P-N(1)}$) in which no two lone pairs (on C(1), N(1), and N(2)) overlap with the same σ^* orbital. It is likely that steric interactions between the *N*-methyl groups in Li^+ 7^- would disfavor a conformation analogous to the C_s local minimum for **4**, although it might be available as an alternate crystalline form.[33] Given the C_s symmetry of the thiophosphoryl analog of Li^+ 1^-, examination of the thiophosphoryl analog of Li^+ 7^- could be informative.[6c]

Comparison to Solution NMR Data. We have discussed in detail the effects of lithiation on the NMR spectra of phosphonic diamides **1**,[6a,21] **2**,[6b,21] and **8**.[11c] The large increase in $^1J_{PC}$ (and $^1J_{CH}$ where appropriate) is indicative of the formation of a planar (sp^2-hybridized) anion from a tetrahedral (sp^3-hybridized) neutral precursor.[34] That increase is observed here as well for Li^+ 7^- (Δ^1J_{PC} = 125.6 Hz and Δ^1J_{CH} = 22.5 Hz (20 °C)). It is thus evident that, in solution as well, these anions are nearly planar.

Although the linearity of the P–O–Li unit (and resulting mechanical restriction on carbon–lithium bonding) was artificially constrained for **6**, it is well-justified given that, in THF solution, no carbon–lithium contact could be detected for Li^+ 1^-, Li^+ 2^-, or Li^+ 7^-.[35] Indeed, this situation facilitated the evaluation of the effect of the lithium cation on the polarization of the phosphonamide unit.

Finally, the rotational dynamics for the anions in solution can also be compared to the theoretical predictions for orientation and energy barrier. In our original communication, were able to set the upper limit to the rotational barrier for Li^+ **2** in THF at ca. 8 kcal/mol on the basis of analysis at –100 °C.[6b] We have now reexamined the ^{13}C NMR spectra of ($^{13}CH_3$)-enriched Li^+ 2^- at ultra-low temperature in dimethyl ether. At –83 °C the isopropyl methyl resonance appeared as a P-coupled doublet at 21.87 ppm (J = 16.5 Hz). Between –83 and –127 °C, the resonance broadened and ultimately decoalesced to a pair of P-coupled doublets (22.89, J = 14.4 Hz; 21.21, J = 17.7 Hz; $\Delta\nu$ = 212 Hz; T_C = –105.1 °C), which translates to a ΔG^*_{rot} = 6.7(±0.6) kcal/mol.[36] Thus, the activation barrier to rotation is as low as initially suggested.

The observation of decoalescence in the ^{13}C NMR spectrum requires that the isopropyl methyl groups are diastereotopic in the rotational ground-state structure of the anion. This establishes the similarity of the anion conformation in the solution and solid-state structures. In addition, the theoretical ground-state structures are in agreement with the experimental observations. For the anion **5** and the derived lithio species **6**, the preferred orientation of the carbanion places the two methylene protons in chemically nonequivalent environments, consistent with the observed anisochronicity of their methyl group analogs in the isopropyl anion at –127 °C. More remarkable, however, is the striking similarity of the rotational barriers: experimental (ΔG^*) Li^+ 7^-, 6.7 kcal/ mol; theoretical (ΔE^*) **5**, 6.7 kcal/mol; **6**, 7.7 kcal/mol. The coincidence of these values is certainly due in part to the fortuitous cancellation of important effects in the experimental determination (e.g., solvation, aggregation, etc.).[37] Moreover, ΔE^* takes into account neither zero-point vibrational energies nor temperature-dependent corrections derived from the

(32) (a) Boche, G.; Marsch, M.; Harms, K.; Sheldrick, G. M. *Angew. Chem., Int. Ed. Engl.* **1985**, *24*, 573. (b) Gais, H.-J.; Vollhardt, J.; Hellmann, G.; Paulus, H.; Lindner, H. J. *Tetrahedron Lett.* **1988**, *29*, 1259.

(33) It is worth noting for **4** that both the C_1 local minimum and the C_1 saddle point are chiral, while their C_s analogs are not. The former, having two interconverting, nonsuperimposable, mirror images, will have an additional $-RT$ ln 2 term contributing to their free energies in solution and will thereby be further stabilized by comparison to the C_s isomers. Nevertheless, the two minima appear to remain close enough in energy that both might contribute to the equilibrium population in solution.

(34) (a) Albright, T. A. *Org. Magn. Reson.* **1976**, *8*, 489. (b) Duangthai, S.; Webb, G. A. *Org. Magn. Reson.* **1983**, *21*, 125. (c) Webb, G. A.; Simonnin, M.-P.; Seyden-Penne, J.; Bottin-Strzalko, T. *Mag. Res. Chem.* **1985**, *23*, 48.

(35) It is noteworthy that the *P*-methyl anion related to Li^+ 1^-, does appear to have a carbon–lithium contact, see ref 21.

(36) Allerhand, A.; Gutowski, H. S.; Jonas, J.; Meinzer, R. A. *J. Am. Chem. Soc.* **1966**, *88*, 3185.

(37) The effect of solvation and aggregation state on rotational dynamics of thiophosphonamide anions has recently been discussed, see ref 6c and d. The aggregation states of Li^+ 1^-, Li^+ 2^-, or Li^+ 7^- in THF solution have been established by $^6Li/^{31}P$ NMR spectroscopy as dimers in all cases. The importance of solvation and aggregation state on rotational dynamics of these compound will be discussed in a full account of those NMR studies, ref 21.

molecular partition functions. On the other hand, none of these latter effects is expected to significantly differentiate between structures of **5** and **6** which differ only as P–C rotamers. In any case, the trend is certainly valid that coordination of the anion by lithium should raise the barrier. By redirecting some of the charge on oxygen to the cation, the acceptor σ^* orbitals on nitrogen are lowered in energy, thus additionally facilitating the stabilizing overlap with the carbanionic lone pair in the rotational ground state.

Finally, it should be mentioned that we have recently demonstrated the ability to electronically modulate the barrier to rotation by attenuating the acceptor properties of the σ^*_{P-X} orbital.[6c] Substitution of sulfur for oxygen in the *thio*phosphonamide analog of Li^+ **2**$^-$ leads to an increased barrier of 9.8 kcal/mol (T_C = –67.6 °C). This can be interpreted by considering the destabilization of the saddle point structure in Figure 8. If the barrier occurs at α = ca. 155°, there is still some stabilization from carbanion lone-pair overlap with the σ^*_{P-O} orbital. Attenuating this stabilization by raising the σ^*_{P-S} orbital in this species apparently results in a net increase in this barrier.

Implications for Synthesis. Most interesting is the suggestion from the theoretical data that the rotational barrier about the P–C bond is sensitive to the nature of the other phosphorus substituents. Thus, the barrier in an acyclic phosphondiamide anion like **4** is expected to be considerably lower than that for a diazaphosphorinane anion like **5** or **6**. Given that this difference may be ascribed to hyperconjugative opportunities present in **4** that are lacking in **5** and **6**, one may imagine synthetic approaches to increasing the P–C rotation barrier by enforcing specific nitrogen lone pair orientations in an appropriate reagent.

In a diazaphospholidine, both nitrogen lone pairs in the now five-membered ring are effectively constrained to be antiperiplanar to the P=O bond (Figure 15). Thus, a conformation placing the carbanion orthogonal to the P=O bond would be expected to be favored and the rotation barrier should be relatively high, since aligning the carbanionic lone pair parallel with the P=O bond effectively removes most of the hyperconjugation into the σ^*_{P-N} orbitals.[38] The individual nitrogen atoms are geometrically prevented from compensating. One may further imagine that distorting the pyramidal nitrogens in opposite directions by virtue of a chiral backbone might significantly bias approach of an electrophile to one face of the carbanion. This hypothesis may well explain the high selectivities observed by Hanessian in anions derived from chiral diazaphospholidines.[4f]

(38) Preliminary theoretical studies on the anion from 2-allyl-1,3,2-diazaphospholidine 2-oxide are in exact accord with this prediction.

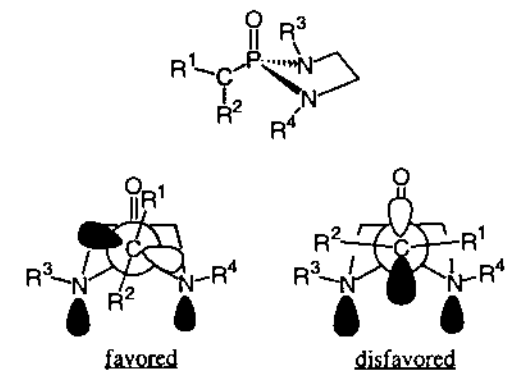

Figure 15. Comparison of hyperconjugative opportunities for a diazaphospholidine-stabilized carbanion. Note that selection of R^3 and R^4 in the favored conformation may allow significant differentiation of the two faces of the carbanion.

Conclusion. In summary, the preferred conformations for phosphondiamide derivative anions are those which maximize opportunities for hyperconjugative stabilization. When the amino substituents in the phosphondiamide are constrained to a diazaphosphorinane-like arrangement, the rotational barrier about the P–C bond is increased and a single local minimum structure is observed. This structure compares well with X-ray single crystal studies of several lithiated phosphondiamides. The relative planarity observed for the unconjugated carbanion in both the theoretical and experimental arenas is unique compared to the cases of other heteroatom-stabilized carbanions. Low rotational barriers in general about the P–C bond are observed in solution in agreement with theoretical predictions. The insights provided by the theoretical analysis offer new concepts for the design of modifier groups.

Acknowledgment. We are grateful to the National Institutes of Health for financial support to S.E.D. (Grant PHS RO1 GM 45521) and to the Army Research Office for financial support to C.J.C. (Grant DAAH04-93-G-0036). P.C.M. thanks the Merck Sharp and Dohme Company for a postdoctoral fellowship. We are grateful to Professor Gernot Boche (Marburg) for a preprint of ref 12.

Supplementary Material Available: Cartesian coordinates for all theoretical structures and positional and thermal parameters along with the details of the X-ray structure determination and a complete listing of bond lengths and angles for Li^+ **7**$^-$ (21 pages). This material is contained in many libraries on microfiche, immediately follows this article in the microfilm version of the journal, and can be ordered from the ACS; see any current masthead page for ordering information.